Aliphatic polyesters as models for relaxation processes in crystalline polymers: 4. Dielectric relaxation in oriented specimens

R. H. Boyd and A. A. Hasan
Department of Materials Science and Engineering and Department of Chemical Engineering, University of Utah, Salt Lake City, Utah, 84112, USA
(Received 25 January 1983; revised 4 April 1983)

To investigate further the effect of the crystal phase on amorphous-phase relaxation, samples of 6–6, 5–7, and 6–10 polyesters have been oriented by extrusion in the solid-state through a tapered die and the dielectric constant and loss measured both parallel and perpendicular to the extrusion direction. The data have been analysed quantitatively in terms of the Cole–Cole phenomenological equation and relaxation times, width parameters and relaxation strengths determined. For the β (glass–rubber relaxation) the relaxation times are shifted 2–3 orders of magnitude to longer times and the relaxation is broadened slightly compared to the unoriented polymers. There also tends to be reduction of overall parallel and perpendicular relaxation strength for the β process on orientation. The γ processes show little effect of orientation on relaxation time and width and do not show reduction of overall relaxation strength. These observations are consistent with crystal displacement further restricting amorphous-phase longer-range segmental motion (β process) but having little effect on the locallized motions associated with the γ process. Both the γ and β processes show anisotropy in relaxation strength. The anisotropy is analysed with a newly developed theory to separate inherent phase anisotropy from apparent anisotropy due to composite or form effects. The average angle made by the lamellar surface normal to the extrusion direction enters as a parameter in the theory. Measurements of relaxed specimen $\varepsilon_{\parallel}$ and $\varepsilon_{\perp}$ values for both the γ and β processes serve to determine both f_a the amorphous-phase orientation function and the average tilt angle for the specimens here. This is possible because for the γ process relaxation strength is small and specimen anisotropy is dominated by inherent phase anisotropy but for the $\gamma+\beta$ processes larger relaxation strength leads to specimen anisotropy being strongly influenced by crystal–amorphous phase composite effects. Values of f_a are in the range of 0.05–0.20 for specimens with f_c in the range 0.5–0.9. Indicated lamellar tilt angles are in the range of 24°–80°.

Keywords Aliphatic polyesters; dielectric relaxation; orientation; crystal phase; amorphous phase; relaxation spectrum

INTRODUCTION

In the previous two papers of the series[1,2], the effect of the presence of the crystalline phase on relaxation processes in the amorphous phase in semicrystalline polymers was studied. Variation of crystallinity, effected over wide limits via copolymerization, was the principal variable assessed. In the present work, the effect of orienting the crystal phase on the relaxations in the amorphous phase are studied as a means of examining the interaction between the phases. In Parts 2 and 3 it was shown that the confinement (folds, loops, tie chains, and restriction of amorphous chain configurations by crystal surfaces) of the amorphous phase by the crystals has a marked effect on relaxation width, broadening the relaxation greatly. Dielectrically it was shown that equilibrium restriction of amorphous chain configurations was manifest in the relaxation strength also. Mechanically it was found that the amorphous fraction has an extremely high relaxed rubbery modulus compared to the unconfined amorphous phase. The displacement of crystal surfaces that accompanies sample orientation during plastic deformation can in principle provide another means for manipulating the dynamic and configurational behaviour of the amorphous fraction (see *Figure 1*). If there were weak coupling between the phases, orientation of the crystal phase carried out well above the glass temperature of the amorphous phase would be expected to have relatively little effect on the relaxation of the latter. However, in the presence of tight coupling and extensive connections between the two, crystal displacement could result in increased immobilization of the amorphous fraction. The latter could be manifested in the displacement of the relaxation to longer times, further broadening of the spectrum and a reduction in relaxation strength.

In the work reported here specimens oriented via solid-state extrusion are studied and the dielectric relaxation measured parallel and perpendicular to the extrusion direction are compared with that in unoriented samples.

Another possible effect of specimen orientation, of course, is the development of orientation in the amorphous phase that would manifest itself as anisotropy in the dielectric constant of this phase. In fact, as the relaxations can be assigned morphologically (amorphous *versus* crystalline) measurement of relaxation anisotropy provides in principle a direct probe into phase anisotropy. The dipole direction in the polyesters is largely normal to the chain axis in the extended planar zig-zag conformation. Hence, if the crystal orientation is accompanied by amorphous chain orientation (favouring extended conformations in the extrusion direction), then a reduction in the dielectric strength associated with amor-

0032-3861/84/030347-10$03.00

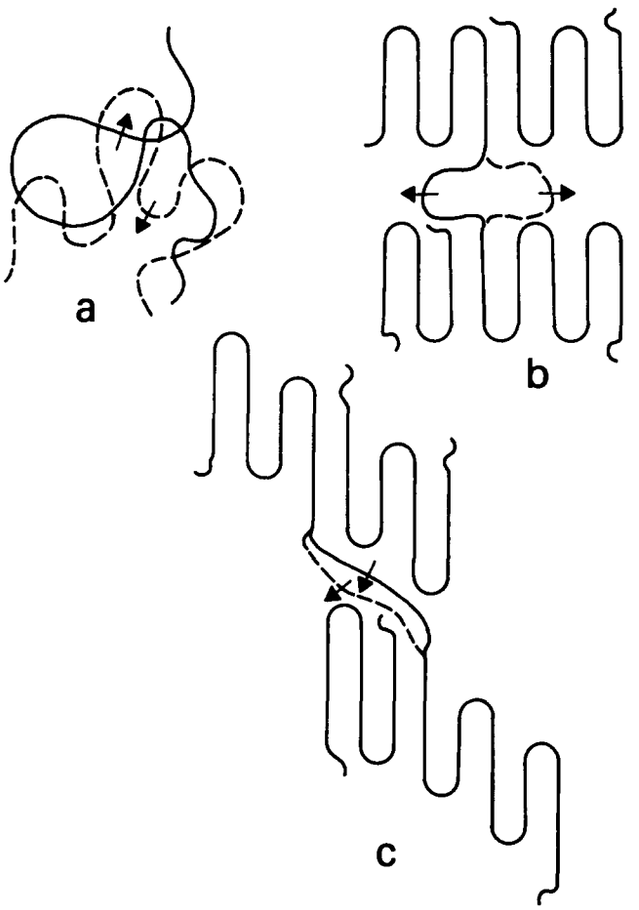

Figure 1 Schematic representation of (a) free amorphous chain relaxation, (b) amorphous chain relaxation confined by crystals, (c) amorphous chain relaxation further restrained due to crystal displacement

phous phase relaxation measured in the parallel direction and an enhancement in the perpendicular one would be expected. These remarks are appropriate when the effects of intramolecular dipole correlation are negligible. As a monitor of this consideration, therefore, both 6–6 and 5–7 polyesters (poly(hexamethylene adipate) and poly-(pentamethylene pimelate) respectively) have been included. In the former the extended conformation tends towards an alternating dipole direction normal to the chain and a reduction in intromolecular dipole correlation factor, whereas the 5–7 tends toward a uniform dipole direction and enhanced intramolecular dipole correlation factor. The detection of anisotropy in the amorphous phase dielectric constant is complicated by crystal–amorphous phase composite effects and it is necessary that these are properly considered. Here, a new theoretical treatment of these effects is used in analysing the data.

EXPERIMENTAL

The general methods used previously[3–5] were followed. An improved 3-terminal guarded parallel-plate cell of 0.5 in (12.7 mm) active electrode diameter was used. Samples were extruded in the solid-state through a tapered die[4] and to a 2 × diameter reduction. Extrusions of 2→1, 1→0.5 and 0.5→0.25 in. could be undertaken. In a number of cases multiple extrusions with succeedingly smaller reductions were made. Two thin samples were cut from each final extruded rod. One had the thin direction (transverse cut) such that the electric field in the dielectric measurement was parallel to the extrusion direction and the other (longitudinal cut) such that the field was perpendicular. For the transverse cut specimen the rod section was first encapsulated in a Teflon cylinder by force fitting the rod in a predrilled hole in the cylinder. The surrounding teflon was left in place after cutting. For the 0.5 in. (12.7 mm) final diameter rods the teflon occupied only the guard ring space. However, for the 0.25 in. (6.35 mm) diameter, the sample occupied only approximately 1/4 of the active electrode area and correction for the Teflon contrbution was made. This, however, seriously degrades the accuracy of the parallel measurements for the 0.25 in. (6.35 mm) rods. This is especially true for absolute values of dielectric constant and less so for comparison loss factor peak heights, etc. The 0.5 in. (12.7 mm) longitudinal cut specimens were not encapsulated. However, for 0.25 in (6.35 mm) samples encapsulation was used. The specimen, after the first of the two cuts, was glued (quick-dry epoxy) to a brass backing plate, then the second cut was made. The plate was left in place during measurement. The Teflon occupied part of the active electrode space but the sample-filled fraction was much higher than for the transverse cut parallel measurements on the 0.25 in. (6.35 mm) rod and the accuracy is not seriously degraded. Conductive silver paint was coated on the surfaces of the specimen before measurement and the samples dried in a vacuum oven. Further details concerning the experimental technique may be found in ref. 6. As considerable importance will be attached to comparison of the parallel and perpendicular measurements, results of measurements made with the cell and sample cutting procedure but carried out as a test on an unoriented molded rod are shown in *Figure 2* and *3*.

The degree of crystal orientation of each sample was determined by X-ray diffraction (flat camera pictures, pin-hole collimation, CuKα radiation). The intensity of a prominent (*hko*) reflection ((210) for 6–6 polyester, (110) for 5–7 polyester and (110) for 6–10 polyester) was measured as a function of azimuth angle, θ_{hko}. The average orientation of the crystallographic *C*-axis with respect to the extrusion direction, θ_c, was computed[6,7] from:

$$\langle \cos^2 \theta_c \rangle = 1 - 2\langle \cos^2 \theta_{hko} \rangle \qquad (1)$$

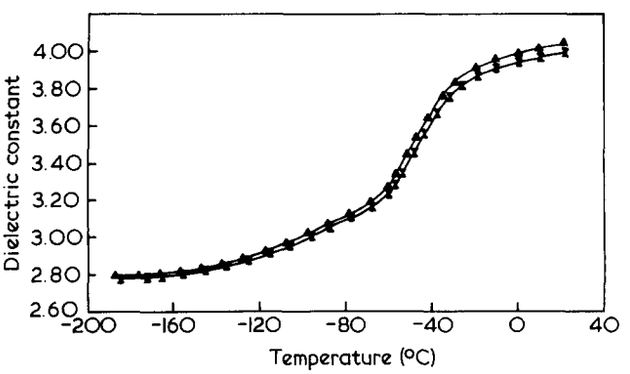

Figure 2 Dielectric constant *versus* temperature (1 kHz) of (x) a parallel and (△) perpendicular measurement of unoriented moulded rod of 6–6 polyester

Then a Hermans orientation function[8]:

$$f_c = \tfrac{1}{2}(3\langle \cos^2 \theta_c \rangle - 1) \quad (2)$$

was calculated.

The extrusion schedules and crystal orientation functions of each specimen studied are summarized in *Table 1*. The crystallinities of the samples were characterized via density (KBr/water density gradient column) and d.s.c. The parameters used for crystallinity calculations are from Part 1[9]: the crystallinity values determined are summarized in *Table 2*.

Attempts were made to determine via small-angle X-ray scattering the orientation of the crystal surfaces with respect to the extrusion direction. However, using pinhole collimation, long path-length, small-angle camera under conditions that produced four-point streaks in polyethylene, no observable pattern could be obtained in long-exposure photographs with the polyesters.

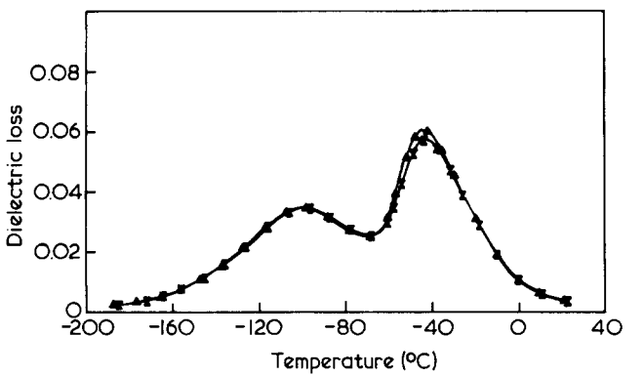

Figure 3 Dielectric loss for same samples as *Figure 2*

Table 1 Solid-state extrusions and degree of orientation

Extrusion designation	Diameter reduction (in)	Extrusion temperature (°C)	Extrusion rate (cm min^{-1})	Degree of orientation (f_c)
6-6 E1	1→0.5	23	0.15	0.58
6-6 E3	1→0.5	15	0.09	0.70
6-6 E4	1→0.5→0.25	23	0.27	0.90
5-7 E1	2→1	18	0.18	0.49
5-7 E2	1→0.5	15	0.08	0.63
5-7 E3	2→1→0.5	15	0.1	0.73
6-10 E1	1→0.5	22	0.17	0.70

RESULTS AND DATA FITTING

Only typical results for the many specimens studied are shown. In *Figures 4* and *5* the dielectric constant and loss factor, respectively. of unoriented 6–6 polyester are shown as isochronal plots *versus* temperature (although the data was taken in isothermal mode). In *Figures 6* and *7* the dielectric constant and loss of 6–6 polyester oriented to $f_c = 0.70$ and measured in the perpendicular (to the

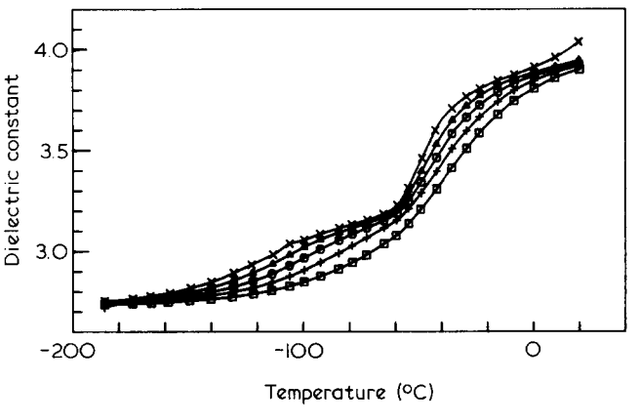

Figure 4 Dielectric constant *versus* temperature of unoriented 6–6 polyester (X, 10 Hz; △, 100 Hz; ○, 1 kHz; +, 10 kHz; □, 100 kHz)

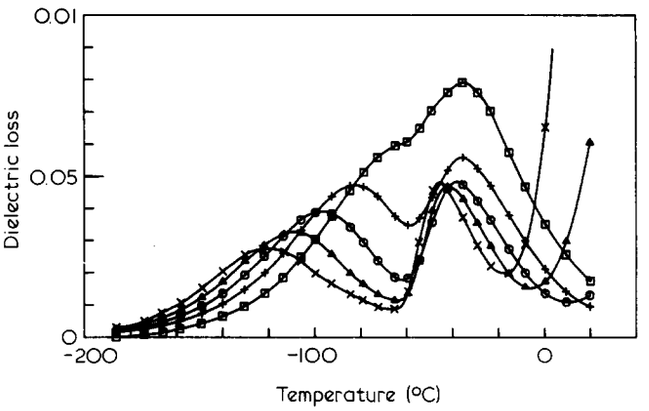

Figure 5 Dielectric loss *versus* temperature for sample in *Figure 4*

Table 2 Crystallinity characterization of studied samples

Sample	Density (g cm^{-3})	Crystallinity based on density	Heat of fusion (J g^{-1})	Crystallinity based on ΔH	Melting point (°C)
6-6 Unoriented	1.160	0.52	78.3	0.52	60
6-6 f_c = 0.58	1.163	0.52	78.7	0.52	58
6-6 f_c = 0.60	1.151	0.44	80.0	0.53	61
6-6 f_c = 0.70	1.158	0.50	81.2	0.54	61
6-6 f_c = 0.90	1.162	0.53	82.9	0.55	61
5-7 Unoriented	1.149	0.48	72.4	0.48	51
5-7 f_c = 0.49	1.151	0.50	86.2	0.57	49
5-7 f_c = 0.63	1.155	0.54	78.3	0.52	49
5-7 f_c = 0.73	1.151	0.50	85.8	0.57	49
6-10 Unoriented	1.099	0.56	74.5	0.56	72
6-10 f_c = 0.70	1.101	0.57	76.6	0.57	71

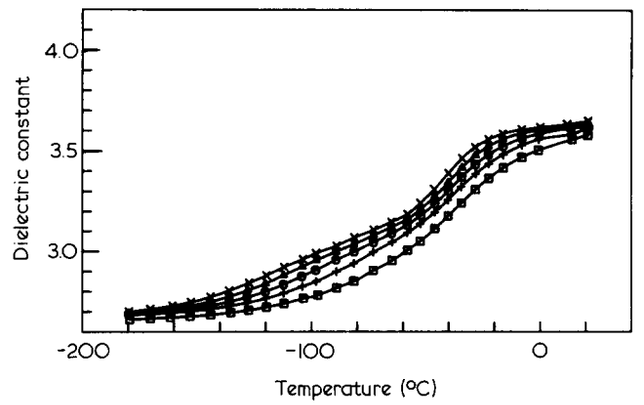

Figure 6 Dielectric constant *versus* temperature of oriented 6–6 polyester (f_c=0.70), perpendicular direction. Same frequencies as *Figure 4*

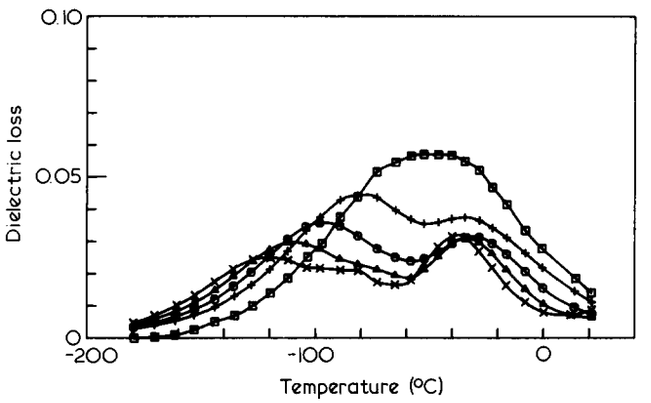

Figure 7 Dielectric loss foe same sample as *Figure 6*

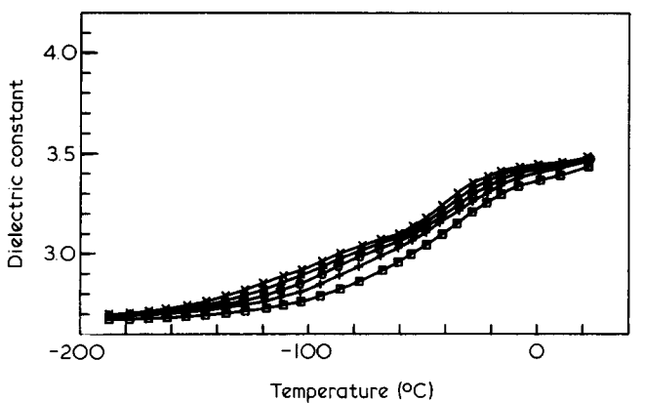

Figure 8 Dielectric constant *versus* temperature of oriented 6–6 polyester (f_c=0.70), parallel direction. Same frequencies as *Figure 4*

extrusion) direction are shown. In *Figures 8* and *9* the results for the same sample measured in the parallel direction are shown. In *Figures 10* and *11* comparison plots at 1 kHz of dielectric constant and loss, respectively, are shown for the unoriented specimen and the perpendicular and parallel measurements on the f_c=0.70 sample. In *Figures 12* and *13* data for unoriented 5–7 polyester are shown and data for unoriented 6–10 polyester is shown in *Figures 14* and *15*.

To facilitate further interpretation, as in Part 2, phenomenological relaxation parameters characterizing the results have been determined. Although it could have been necessary to use the full Havriliak–Negami[10] equation, it was established that the results required only symmetrical broadening so that the Cole–Cole[11] function could be used and the relaxation was fitted to:

$$\varepsilon^* = \varepsilon_U + (\varepsilon_U - \varepsilon_R)_1/[1 + (i\omega\tau_1)^{\bar{\alpha}_1}] + (\varepsilon_U - \varepsilon_R)_2/[1 + (i\omega\tau_2)^{\bar{\alpha}_2}] \quad (3)$$

where U, R refer to unrelaxed and relaxed values, respectively, ω to angular frequency, τ to central relaxation time, $\bar{\alpha}$ to the broadening parameter and 1, 2 to the γ and β processes, respectively. The same forms for the temperature dependence of the parameters as in Part 2

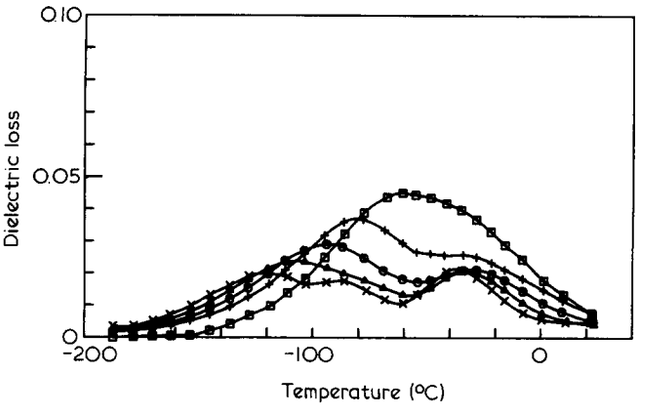

Figure 9 Dielectric loss for same sample as *Figure 8*

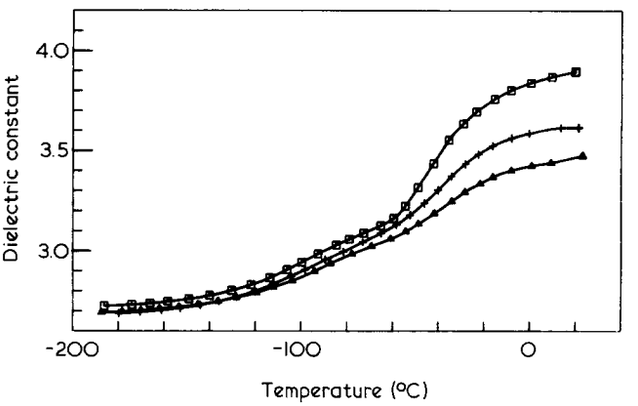

Figure 10 Dielectric constant of unoriented (□) 6–6 polyester compared with oriented (f_c=0.70) perpendicular (+) and parallel (△) samples at 1 kHz

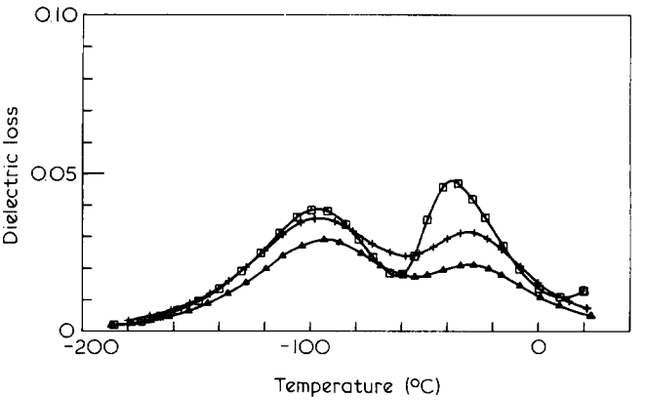

Figure 11 Dielectric loss of samples in *Figure 10*

were involved (equations (2a–e) of Part 2). The same fitting procedure was used[1,6]. One slight change, however, was made. It was noticed that slightly better fits could be obtained if the broadness parameter, $\bar{\alpha}$, for the γ process was allowed to increase more rapidly above T_g (where the low frequency side of the γ process overlaps the β process) than below it. Hence, two linear segments of differing slope but coincident at $T = 200$ K were used to represent the temperature dependence of $\bar{\alpha}$ for the γ process. Considerable more conductance related, Maxwell–Wagner loss was found at high temperatures above the process for the 5–7 polyesters than in the 6–6 or 6–10 polyesters (*cf. Figures 12, 13* with *4, 5* or *14, 15*). This led to lower accuracy in the ε_R values for the β process for the 5–7 polyesters. All of the resulting parameters are listed in *Tables 3* and *4*. An illustrative fit is shown in *Figures 16*

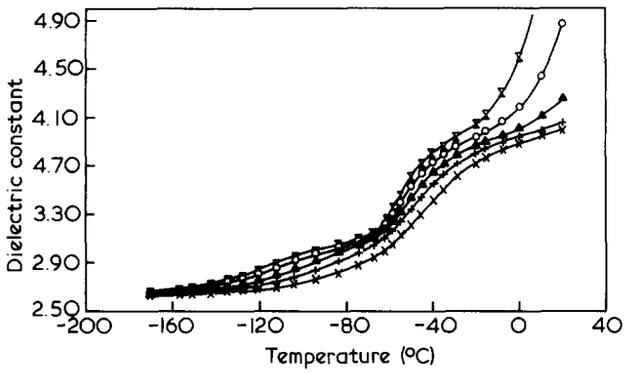

Figure 12 Dielectric constant *versus* temperature of unoriented 5–7 polyester. x, 10; ○, 100; ▲, 1000; +, 10000; *, 100000 Hz

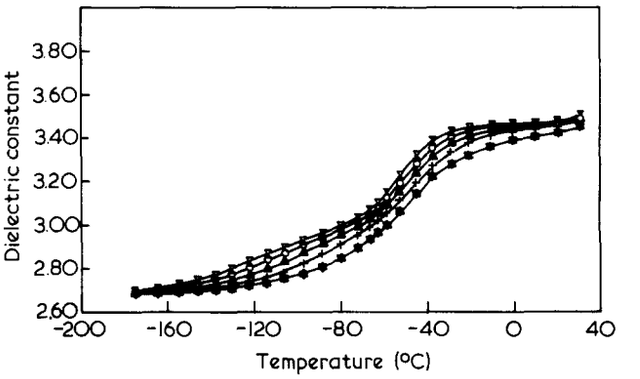

Figure 14 Dielectric constant *versus* temperature of unoriented 6–10 polyester. Same frequencies as *Figure 12*

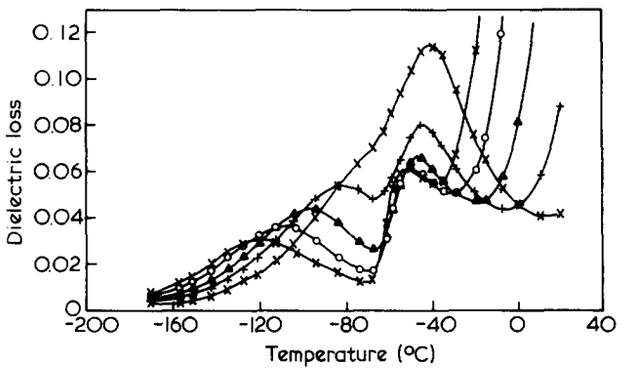

Figure 13 Dielectric loss *versus* temperature of unoriented 5–7 polyester. Same frequencies as *Figure 12*

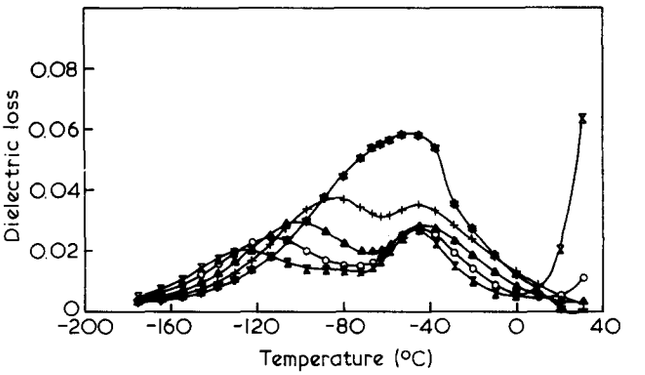

Figure 15 Dielectric loss *versus* temperature of unoriented 6–10 polyester. Same frequencies as *Figure 12*

Table 3 Cole–Cole phenomenological parameters for the γ process[a]

		ϵ_U		ϵ_R		$\bar{\alpha}$, $T < 200$ K		$\bar{\alpha}$, $T > 200$ K		log τ	
Sample		ϵ_U	S_U	ϵ_R	S_R	α_0	α'	α_0	α'	A	$-B$
6-6 Unoriented		2.75	0.0000	3.10	0.0020	0.303	0.0026	0.373	0.0039	2103	16.53
6-6 $f_c = 0.58$	∥	2.70	0.0000	3.01	0.0016	0.272	0.0025	0.340	0.0027	2444	18.54
6-6 $f_c = 0.58$	⊥	2.72	0.0000	3.09	0.0023	0.278	0.0029	0.357	0.0063	2171	16.92
6-6 $f_c = 0.70$	∥	2.69	0.0001	2.98	0.0023	0.264	0.0019	0.317	0.0035	1966	15.88
6-6 $f_c = 0.70$	⊥	2.67	0.0000	3.03	0.0030	0.256	0.0013	0.290	0.0049	1952	15.91
6-6 $f_c = 0.90$	∥[b]	(2.60)	(–0.0001)	(2.87)	(0.0015)						
6-6 $f_c = 0.90$	⊥	2.60	–0.0001	2.98	0.0015	0.292	0.0036	0.390	0.0036	2000	16.43
5-7 Unoriented		2.63	0.0000	3.02	0.0016	0.295	0.0031	0.379	0.0031	2467	18.74
5-7 $f_c = 0.49$	∥	2.74	0.0000	3.10	0.0021	0.278	0.0021	0.334	0.0063	2229	17.38
5-7 $f_c = 0.49$	⊥	2.74	0.0000	3.14	0.0027	0.279	0.0023	0.342	0.0042	2225	17.17
5-7 $f_c = 0.63$	∥	2.70	0.0002	3.05	0.0026	0.265	0.0022	0.323	0.0068	2240	17.23
5-7 $f_c = 0.63$	⊥	2.83	0.0000	3.29	0.0040	0.289	0.0023	0.352	0.0058	2061	16.16
5-7 $f_c = 0.73$	∥	2.72	–0.0001	3.12	0.0018	0.266	0.0027	0.339	0.0057	2274	17.51
5-7 $f_c = 0.73$	⊥	2.74	–0.0004	3.21	0.0029	0.264	0.0021	0.321	0.0053	2344	17.85
6-10 Unoriented		2.67	–0.0001	2.95	0.0020	0.302	0.0020	0.355	0.0059	1870	15.59
6-10 $f_c = 0.70$	∥	2.65	0.0000	2.94	0.0025	0.280	0.0016	0.322	0.0047	2112	16.60
6-10 $f_c = 0.70$	⊥	2.68	0.0001	3.04	0.0031	0.303	0.0086	0.347	0.0086	1778	14.94

[a] Parameters for equation (3) of text; ϵ_U^0, ϵ_R^0 are the unrelaxed and relaxed dielectric constants at 173 K, S_U, S_R their temperature coefficients; α_0 is width parameter at 173 K, α' its temperature coefficient (additional set for α_0 at 200 K for $T > 200$ K is also given); $\log \tau = A/T + B$

[b] See text for discussion

Table 4 Cole–Cole phenomenological parameters for the β process[a]

Sample		e_U		e_R		$\bar{\alpha}$		log τ		
		e_U^0	S_U	e_R	S_R	α	α'	A	$-B$	T_∞ (K)
6-6 Unoriented		3.20	0.00198	3.90	0.0000	0.170	0.0000	1614.0	22.48	150
6-6 f_c = 0.58	∥	3.09	0.0016	3.51	−0.0003	0.130	0.0006	1267.0	20.67	170
6-6 f_c = 0.58	⊥	3.21	0.0023	3.70	−0.0003	0.140	0.0011	639.2	14.92	190
6-6 f_c = 0.70	∥	3.09	0.0023	3.51	−0.0009	0.135	0.0009	2491.0	26.73	140
6-6 f_c = 0.70	⊥	3.18	0.0030	3.65	−0.0002	0.180	0.0002	715.1	14.40	180
6-6 f_c = 0.90	∥[b]	(2.95)	(0.0015)	(3.38)	0.0004					
6-6 f_c = 0.90	⊥	3.05	0.0015	3.60	0.0004	0.119	0.0017	729.8	13.83	180
5-7 Unoriented		3.10	0.0016	4.00	0.0000	0.167	0.0008	512.7	14.58	180
5-7 f_c = 0.49	∥	3.20	0.0020	3.96	−0.0002	0.149	0.0005	586.5	14.48	180
5-7 f_c = 0.49	⊥	3.28	0.0027	4.23	0.0017	0.135	0.0006	650.6	13.15	180
5-7 f_c = 0.63	∥	3.18	0.0027	3.80	−0.0002	0.126	0.0005	794.9	16.26	180
5-7 f_c = 0.63	⊥	3.49	0.0040	4.34	0.0011	0.150	0.0000	645.1	14.20	180
5-7 f_c = 0.73	∥	3.21	0.0018	3.81	0.0000	0.144	0.0002	591.7	13.00	180
5-7 f_c = 0.73	⊥	3.35	0.0028	4.30	0.0000	0.142	0.0005	2303.0	26.16	140
6-10 Unoriented		3.04	0.0020	3.50	−0.0003	0.146	0.0004	1125.0	19.23	160
6-10 f_c = 0.70	∥	3.06	0.0025	3.48	−0.0013	0.092	0.0009	4748.0	36.85	100
6-10 f_c = 0.70	⊥	3.19	0.0031	3.69	−0.0008	0.136	0.0005	594.6	13.90	180

[a] Parameters for equation (3) of text; e_U^0, e_R^0 are the unrelaxed and relaxed dielectric constants at 223 K, S_U, S_R their temperature coefficients, α_0 is width parameter at 223 K, α' its temperature coefficient; $\log \tau = A/(T - T_\infty) + B$

[b] See text for discussion

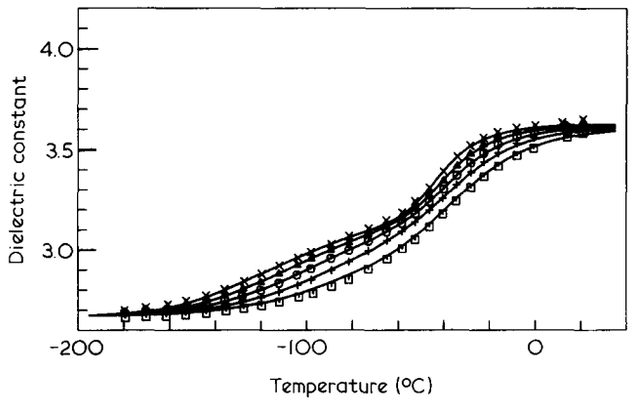

Figure 16 Fitting of data with Cole–Cole phenomenological equations. Dielectric constant of perpendicular 6–6 polyester (f_c=0.70). Points are experimental, curves are calculated from equation (3) of text and parameters of *Tables 3* and *4*

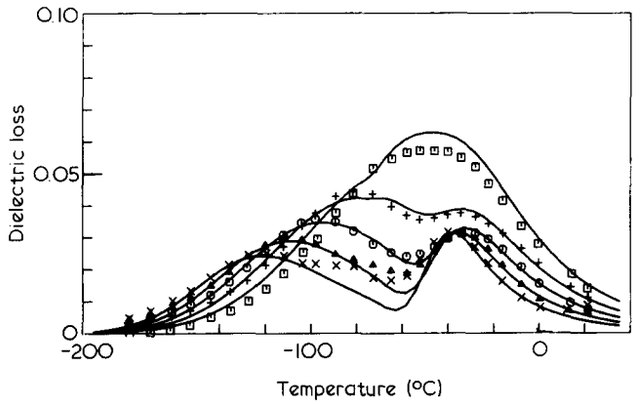

Figure 17 Fitting of data with Cole–Cole phenomenological equations. Dielectric loss of perpendicular 6–6 polyester (f_c=0.70). Points are experimental, curves are calculated from equation (3) of text and parameters of *Tables 3* and *4*

and *17*. The results for the 6–6 polyester with f_c=0.90 were obtained on a specimen of 0.25 in. (6.35 mm) diameter and, as was explained previously the parallel measurement is not of as high accuracy, especially with

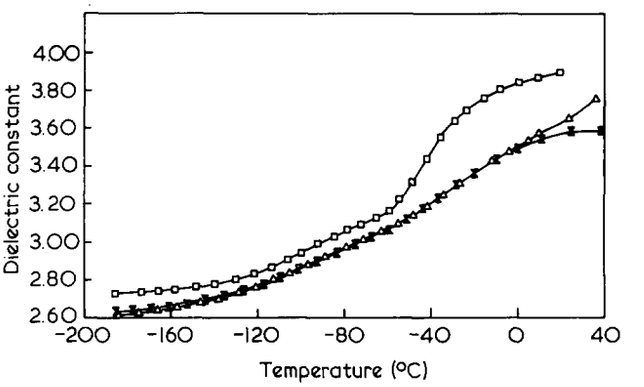

Figure 18 Dielectric constant of unoriented 6–6 polyester (□) compared with oriented (f_c=0.90) perpendicular (▲) and parallel (x) samples at 1 kHz

respect to absolute values of dielectric constants, as the other measurements. Comparison plots of dielectric constants and loss for the perpendicular and parallel measurements for this specimen are shown in *Figures 18* and *19*. For the parallel measurement, the relaxation strength of the γ process, $\varepsilon_R - \varepsilon_U$, was taken to be 0.72 (the ratio of parallel and perpendicular ε''_{max} values in *Figure 19*) times that of the perpendicular measurement and ε_U was taken to be the same. As the width parameters, $\bar{\alpha}$, are very similar in the two directions for other specimens (*Table 3*) for the γ process this should be a very good approximation. For the β process the analogous procedure has been followed but it is not as certain as there is a tendency (*Table 4*) for the 6–6 and 6–10 polyesters to have lower $\bar{\alpha}$ values in the parallel direction than in the perpendicular.

DISCUSSION

Dynamics

First the effect of crystal orientation on the location (central relaxation time τ) and shape (width parameter $\bar{\alpha}$) of the amorphous phase β and γ relaxations is examined.

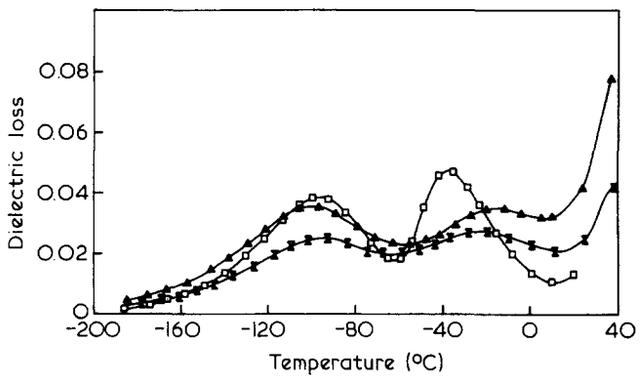

Figure 19 Dielectric loss of unoriented 6–6 polyester (□) compared with oriented (f_c=0.90) perpendicular (▲) and parallel (x) samples at 1 kHz

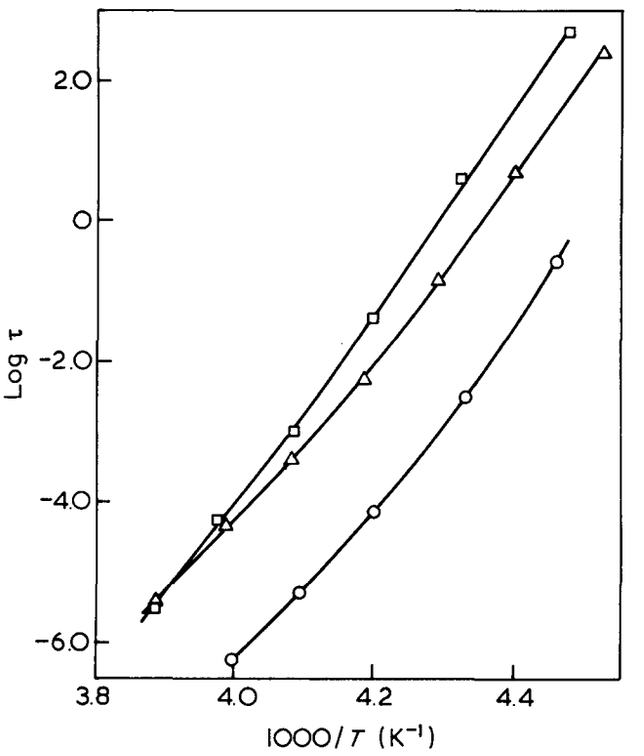

Figure 20 Log of Cole–Cole relaxation time, τ, for the β process *versus* $1/T$ for unoriented (○) 6–6 polyester and parallel (□) and perpendicular (△) 6–6 polyester, f_c=0.70. The points are from isothermal fitting procedure and curves are calculated from parameters of *Table 3*

In contrast to the copolymer studies (in Part 2) where the effect of changing crystallinity on τ is obscured by changes in the chemical composition, here the effect of crystal orientation on τ is readily observed. Discussing the glass–rubber β relaxation first, *Figure 20* is a plot of log τ *versus* $1/T$ for the 6–6 polyester oriented to f_c=0.70 (same specimen as shown in *Figures 4–9*). It is evident that the relaxation time is shifted to larger values for both the ⊥ and || directions in the oriented specimen (approximately 2–3 orders of magnitude). This result is typical of all of the samples. There is a good correlation between the degree of crystal orientation (f_c) and the relaxation time shift in the || direction for all of the specimens. This is not the case for the ⊥ direction where the amount of shift with orientation is more erratic. The width parameter for the same specimens are plotted in *Figure 21*. It is evident that there is not a marked effect of crystal orientation on the β process relaxation width. However, the parallel direction does have a lower $\bar{\alpha}$ value and *Table 4* indicates a general tendency for the $\bar{\alpha}$ values for both directions to be lower in the extruded samples than in the unoriented.

Turning to the γ process, *Figure 22* for the same specimens (6–6 polyester, f_c=0.70) shows that the relaxation times are very similar in both the unoriented and extruded samples. In general for the specimens in *Table 3* there is very little effect of crystal orientation on the γ process relaxation times. In *Figure 21* it is evident that for this specimen the width parameter $\bar{\alpha}$ for the γ process is not very sensitive to extrusion. *Table 3* shows that, in general, the γ process width has a slight but discernable trend toward broadening an orientation of the samples.

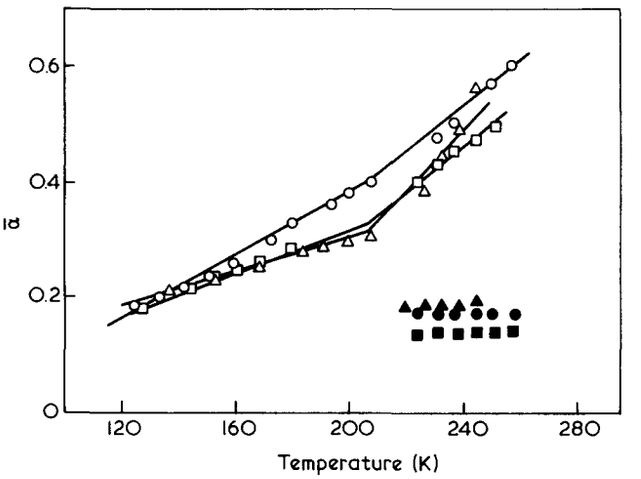

Figure 21 Cole–Cole width parameter $\bar{\alpha}$ for γ process unoriented 6–6 polyester (○), and parallel (□) and perpendicular (△) 6–6 polyester; filled symbols are for β process

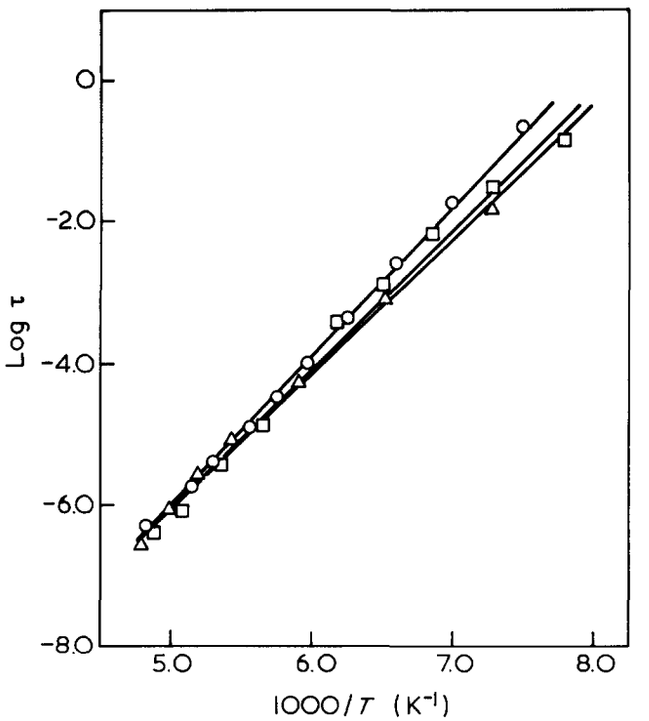

Figure 22 Log of Cole–Cole relaxation time, τ, for the γ process *versus* $1/T$ for unoriented 6–6 polyester (○) and parallel (□) and perpendicular (△) 6–6 polyester, f_c=0.70

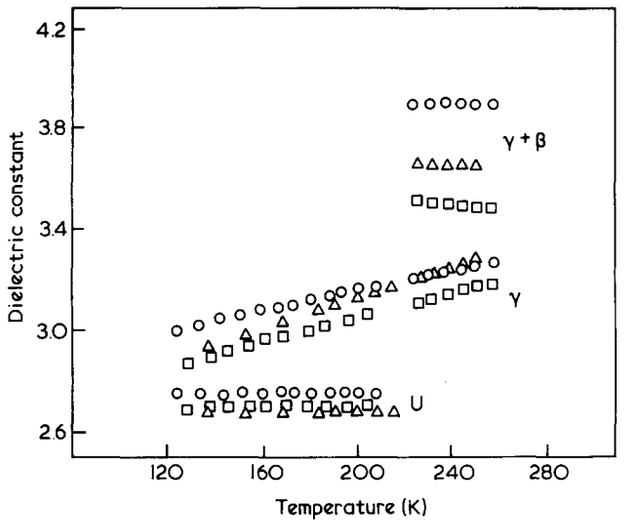

Figure 23 Relaxation strengths for γ and $\gamma+\beta$ processes in unoriented (○) 6–6 polyester and parallel (□) and perpendicular (△) 6–6 polyester, $f_c=0.70$

It is now possible to summarize the effect of crystal orientation on the γ and β process dynamics. For the β process the process shifts significantly (but not dramatically, i.e. 2–3 orders of magnitude in τ) to longer times with crystal orientation. This is accompanied by some broadening. In contrast, the γ process is relatively insensitive to the orientation process. These observations are consistent with the β process as a glass–rubber relaxation involving long-range segmental motions sensitive to connections to and immobilization by the crystals and the γ process in contrast involving more locallized motions that are insensitive to the crystal connections.

Relxation strength and anisotropy

Part of the aim of this work was to establish the extent to which crystal orientation affects availability of amorphous chain configurations and to what extent orientation of the amorphous fraction is indicated by the relaxation processes. In *Figure 23* the relaxed and unrelaxed dielectric constants *versus T* are plotted for the γ and $\gamma+\beta$ processes for 6–6 polyester, $f_c=0.70$. Inspection of this plot as well as the data directly (*Figure 10, 11*) shows two features. First there is indeed noticeable *apparent* or *specimen* anisotropy. The parallel measurements have a lower relaxation strength (and also $\varepsilon_{\max}$. as $\bar{\alpha}$ values are similar) than the perpendicular ones for both the γ and β processes. This effect is confirmed for all the specimens (*Tables 3* and *4*). The second observation is that the specimens (*Figure 23*) tend to show reduction in the β relaxation strength in *both* the perpendicular and parallel directions compared to the unoriented specimen. The reduction seems less pronounced in the 5–7 polyester. However, because the 5–7 samples show more Maxwell–Wagner conductance effects the relaxed $\gamma+\beta$ dielectric constants (especially in the $\perp$ direction) are not as accurately quantified as in the 6–6 polyesters. In the γ process there appears to be little effect of orientation in increasing or decreasing relaxation strength beyond the development of specimen anisotropy (*Figure 23*). The reduction in relaxation strength on specimen orientation for the β process is consistent with the notion that crystal displacement results in further restriction on amorphous-phase, long-range segmental motion. The insensitivity of the γ process relaxation strength to crystal orientation again is indicative of short-range or localized motions.

Turning now to the question of anisotropy induced in the amorphous phase by crystal orientation it is necessary to clarify the distinction between sample anisotropy and phase anisotropy and the following illustration is helpful. In a semi-crystalline specimen of lamellar structure that is completely oriented with the lamellar surfaces normal to the extrusion direction, the dielectric constant in the perpendicular direction ($\perp$) to the extrusion direction is:

$$\varepsilon_\perp=(1-x)\varepsilon_{1_\perp}+x\varepsilon_2 \tag{4}$$

and in the parallel direction it is:

$$1/\varepsilon_\parallel=(1-x)/\varepsilon_{1_\parallel}+x/\varepsilon_2 \tag{5}$$

where 1 and 2 refer to the amorphous and crystalline phases, respectively, and x is the volume fraction crystallinity. As there is no relaxation process in the crystals they are non-polar and to a good approximation isotropic ($\varepsilon_{2_\perp}=\varepsilon_{2_\parallel}=\varepsilon_2$). Even if the amorphous phase is isotropic ($\varepsilon_{1_\parallel}=\varepsilon_{1_\perp}=\varepsilon_1$), $\varepsilon_\parallel$ will be less than $\varepsilon_\perp$ and there will be *apparent* or *specimen* anisotropy. This effect is the same phenomenon as 'form' birefrigence in optical measurements. The greater the difference in ε_1 and ε_2 the greater the apparent anisotropy in $\varepsilon_\parallel$ and $\varepsilon_\perp$. These equations are valid only for a completely oriented material of the type described. Recently, it has been shown[12] that relatively tight bounds to $\varepsilon_\parallel$ and $\varepsilon_\perp$ in an incompletely oriented specimen of lamellar structure can be found. If the individual phases are anisotropic, this treatment requires generalization and this has been carried out in a separate development[13]. The resulting equations as applied here (summarized in the Appendix) permit the determination of the amorphous-phase dielectric constant parallel ($\varepsilon_{1_\parallel}$) and perpendicular ($\varepsilon_{1_\perp}$) to the extrusion direction from measured specimen values $\varepsilon_\parallel$, $\varepsilon_\perp$, the degree of crystallinity, the crystal phase dielectric constant and the average lamellar surface orientation. If the lamellar surfaces are normal to the crystallographic c-axes then the experimentally measured c-axis orientation function, f_c, would serve to characterize the orientation of the surfaces. However, it is likely that in more highly oriented specimens the lamellar surface normals are tilted with respect to the c-axes and extrusion direction. Thus, another parameter, the average lamellar surface tilt angle is required. In extremely highly oriented specimens it is probably not appropriate to describe the morphology as lamellar but rather as more fibrillar in nature. However, even here the lamellar description by adopting an extreme angle of surface tilt, one that is closer to 90° than 0°, should provide a useful approximation. As the lamellar surface orientation could not be measured successfully using small-angle X-ray scattering, the average tilt angle remains an independent parameter. However, the experimental values of $\varepsilon_\perp$ and $\varepsilon_\parallel$ can be used to determine the amorphous-phase values $\varepsilon_{1_\perp}$ and $\varepsilon_{1_\parallel}$ as well as the average tilt angle; because there are two sets of parallel and perpendicular relaxation strengths available, one for the γ process and one for the β process. To show this, a convenient measure of amorphous-phase anisotropy is used.

$$f_a=2[3\Delta\varepsilon_{1_\perp}/(2\Delta\varepsilon_{1_\perp}+\Delta\varepsilon_{1_\parallel})-1] \tag{6}$$

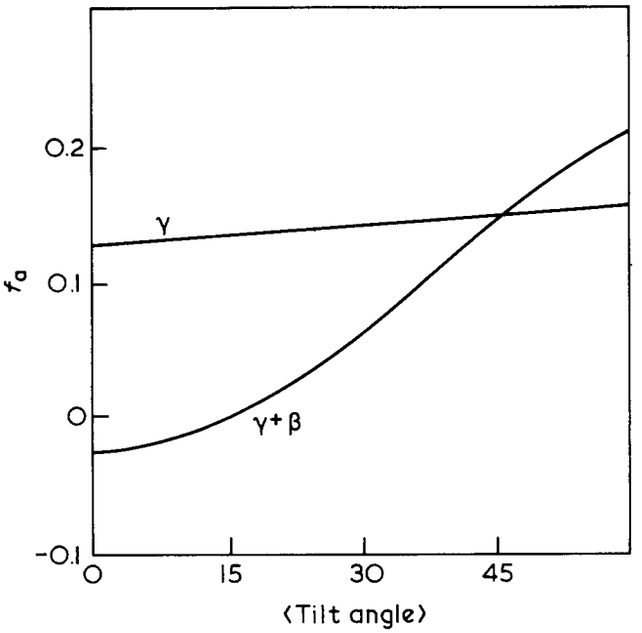

Figure 24 Derived amorphous-phase orientation function, f_a for 6–6 polyester, $f_c=0.70$, *versus* possible average angle of lamellar normals to extrusion direction. Curve labelled γ is calculated from γ process || and ⊥ relaxation strengths, curve labelled $\gamma+\beta$ from || and ⊥ $\gamma+\beta$ relaxation strengths

where $\Delta\varepsilon_{1_\perp}=\varepsilon_{1_\perp}-\varepsilon_{1_U}$, $\Delta\varepsilon_{1_\parallel}=\varepsilon_{1_\parallel}-\varepsilon_{1_U}$ and ε_{1_U} is the unrelaxed amorphous-phase dielectric constant, assumed to be isotropic. In a dilute dipole system where direct dipole–dipole correlations vanish, f_a is an Herman's orientation function for chain direction when the dipole direction is normal to the chain.[14–17] In the work on unoriented polyesters (Part 2) there was no evidence of an intramolecular dipole correlation and at the low degrees of amorphous-phase anisotropy found here it is reasonable to suppose that f_a is a true orientation function for chain direction. As stated previously, values of $\varepsilon_{1_\parallel}$ and $\varepsilon_{1_\perp}$ may be calculated from the specimen values of $\varepsilon_\parallel$ and $\varepsilon_\perp$ (relaxed values in *Tables 3* and *4*) as a function of average tilt angle. Values of ε_{1_U} were derived from the ε_U values of *Table 3* by the same Clausius–Mosotti density correction method described in Part 2. Values of f_a for the γ process as a function of possible values of the average lamellar surface tilt angle are shown for the 6–6 polyester specimen with $f_c=0.70$ in *Figure 24*. It is apparent that for the γ process f_a is relatively insensitive in the tilt angle. This is because the relaxation strength is small for the γ process and the crystal and amorphous-phase dielectric constants are not very different. Thus, the 'composite' or 'from effects' are relatively minimal. The specimen anisotropy is mostly directly due to amorphous-phase anisotropy. For the $\gamma+\beta$ process the situation is different. The orientation function $f_a(\gamma+\beta)$ is also shown in *Figure 24* and in this case it is very sensitive to the possible values of tilt angle. This is because the relaxation strength is much higher, the amorphous- and crystal-phase dielectric constants much more disparate, and specimens $\varepsilon_\parallel$, $\varepsilon_\perp$ are anisotropy of a specimen at a constant value, the f_a values must increase markedly with tilt angle. As it is probable tgat $f_a(\gamma)$ and $f_a(\gamma+\beta)$ are good approximations to true chain orientation functions they must have identical values. Thus, the crossover point in *Figure 24* defines both f_a and the average tilt angle. The values of f_a and tilt angle

Table 5 Crystal- and amorphous-phase orientation functions and average lamellar tilt angle

Sample	f_c	f_a	⟨Tilt angle⟩
6-6 E1	0.58	0.12	45°
6-6 E3	0.70	0.15	48°
6-6 E4	0.90	0.18	80°
5-7 E1	0.49	0.05	24°
5-7 E2	0.63	0.15	35°
5-7 E3	0.73	0.07	33°
6-10 E1	0.70	0.16	48°

determined for all of the samples are shown in *Table 5*. There is some correlation between the degree of amorphous-phase orientation and the average tilt angle. For the most highly oriented specimen, the 6–6 polyester extruded to 0.25 in. (6.35 mm) diameter, resulting in $f_c=0.90$ the tilt angle is approaching 90° presumably indicating a transition to a fibrillar morphology.
determined for all of the samples are shown in *Table 5*. There is some correlation between the degree of amorphous-phase orientation and the average tilt angle. For the most highly oriented specimen, the 6–6 polyester extruded to 0.25 in. (6.35 mm) diameter, resulting in $f_c=0.90$ the tilt angle is approaching 90° presumably indicating a transition to a fibrillar morphology.

Relation to other polymers

Studies of $\varepsilon_\parallel$, $\varepsilon_\perp$ in oriented specimens have been carried out on the γ process in slightly oxidized linear (LPE) and branched (BPE) polyethylenes[3] and poly(chlorotrifluoroethylene)[18], the β process in BPE[3], the α process ($=\beta$ process in polyesters here) in aliphatic polyamides[4,5] and the α (crystalline) process in BPE and LPE[3]. In PE the amorphous- and crystalline-phase dielectric constants are very similar so that composite effects essentially vanish. Judging from the $\varepsilon^\parallel_{max}$ values associated with the γ process in PE (relaxation strengths were not reported) the aliphatic polyesters studied here appear to be intermediate in the extent of amorphous-phase orientiation between BPE and LPE (the f_c values are probably similar), the anisotropy being slight in BPE ($f_a\approx0.05$) but $f_a\approx0.3$ in LPE. The β process in BPE shows similar behaviour to the γ process because form effects vanish. The β process in LPE is not clearly resolved. For the γ process in PCTFE, Choy *et al.*[18] report $f_a=0.3$–0.4 for f_c values in the range studied here (0.6–0.7). However, no corrections for morphological composite effects were attempted. In the α (glass–rubber relaxation) in oriented aliphatic polyamides there is extreme anisotropy in the measured $\varepsilon_\perp$, $\varepsilon_\parallel$. This no doubt is a good example of the apparent anisotropy being dominated by composite effects as the phase dielectric constants are significatly different. Reduction in both $\varepsilon_\perp$ and $\varepsilon_\parallel$ relative to the unorienated samples indicating further restrictions of amorphous configurations on crystal orientation is found in the polyamides as it was here for the polyesters. Finally, it is to be noted that the α (crystalline) process in polyethylenes shows[3] just the anisotropy expected for dipoles perpendicular to the *c*-axis in the crystals undergoing re-orientation and this behaviour, in fact, forms one of the key pieces of evidence, regarding the mechanism for the α process.[20].

ACKNOWLEDGEMENT

The authors are indebted to the National Science Foundation, Division of Materials Research, Polymers Program (DMR 80-18326) for financial support of this work.

REFERENCES

1 Boyd, R. H. and Aylwin, P. A. *Polymer* 1984, **25**, 330
2 Boyd, R. H. and Aylwin, P. A. *Polymer* 1984, **25**, 340
3 Boyd, R. H. and Yemni, T. *Polym. Sci. and Eng.* 1979, **19**, 1023
4 Yemni, T. and Boyd, R. H. *J. Polym. Sci.-Polym. Phys. Ed.* 1976, **14**, 499
5 Yemni, T. and Boyd, R. H. *J. Polym. Sci.-Polym. Phys. Ed.* 1979, **17**, 741
6 Hasan, A. A. *Ph.D. Dissertation* University of Utah, 1982
7 Wilchinsky, Z. W. 'Advances un X-Ray Analysis', Vol. 6, Plenum Press, New York, 1963
8 Hermans, J. J., Hermans, P. H., Vermaas, D. and Weidinger, A. *Rec. Trav. Chim. Pays-Bas* 1946, **65**, 427
9 Aylwin, P. A. and Boyd, R. H. *Polymer* 1984, **25**, 323
10 Havriliak, S. and Negami, S, S. S. *Polymer* 1967, **8**, 161
11 Cole, K. S. and Cole, R. H. *J. Chem. Phys.* 1941, **9**, 341
12 Boyd, R. H. *J. Polym. Sci.-Polym. Phys. Edn* 1983, **21**, 505
13 Boyd, R. H. *Macromol.* in press
14 Bares, J. *Koll. Z. Z. Polym.* 1970, **239**, 552
15 Phillips, P. J., Kleinheins, G. and Stein, R. S. *J. Polym. Sci. A-2* 1972, **10**, 1593
16 Lau, K. H. and Young, K. *Polymer* 1975, **16**, 477
17 Lau, K. H. and Young, K. *Polymer* 1976, **17**, 7
18 Choy, C. L., Cheng, K. H. and Hsu, B. S. *J. Polym. Sci.-Polym. Phys. Ed.* 1981, **19**, 991
19 McCullough, R. L. 'Treatise on Materials Science and Technology', Vol. 10—Part B (Ed. J. M. Schultz) Academic Press, New York, 1977
20 Mansfield, M. and Boyd, R. H. *J. Polym. Sci.—Polym. Phys. Ed.* 1978, **16**, 1227

APPENDIX

In a semi-crystalline polymer with morphology consisting of layers of stacked lamellae the dielectric tensor ε of a local region can be written as[13]:

$$\varepsilon=\begin{pmatrix}\varepsilon_{11} & 0 & \varepsilon_{13}\\ 0 & \varepsilon_{22} & 0\\ \varepsilon_{13} & 0 & \varepsilon_{33}\end{pmatrix} \tag{A-1}$$

where:

$$\varepsilon_{11}=(1-x)\varepsilon_{1_\perp}\cos^2\theta+\varepsilon_{1_\parallel}\sin^2\theta)+x\varepsilon_2$$

$$\varepsilon_{22}=(1-x)\varepsilon_{1_\perp}+x\varepsilon_2$$

$$\varepsilon_{13}=-(1-x)\left(\frac{1}{\varepsilon_{1_\parallel}}-\frac{1}{\varepsilon_{1_\perp}}\right)\sin\theta\cos\theta\,\varepsilon_{1_\perp}/[A]$$

$$\varepsilon_{33}=1/[A]+\varepsilon_{11}\left[(1-x)\left(\frac{1}{\varepsilon_{1_\parallel}}-\frac{1}{\varepsilon_{1_\perp}}\right)\sin\theta\cos\theta/[A]\right]^2$$

$$[A]=(1-x)\left(\frac{1}{\varepsilon_{1_\parallel}}\cos^2\theta+\frac{1}{\varepsilon_{1_\perp}}\sin^2\theta\right)+\frac{x}{\varepsilon_2}$$

and $\varepsilon_{1_\parallel}$, $\varepsilon_{1_\perp}$ are the amorphous-phase dielectric constants parallel and perpendicular to the extrusion direction; ε_2 is the dielectric constant of the crystal phase (assumed to be isotropic); x is the degree of crystallinity and θ is the angle made by the normal to the lamellar surfaces with the extrusion direction. Spatial averaging under axial symmetry of equation (A-1) for various orientations of the local regions to the extrusion direction leads to upper bounds to the specimen constant in the parallel and perpendicular directions as:

$$\varepsilon_\parallel=\langle\varepsilon_{33}\cos^2\theta\rangle+2\langle\varepsilon_{13}\sin\theta\cos\theta\rangle+\langle\varepsilon_{1_\perp}\sin^2\theta\rangle \tag{A-2}$$

$$\varepsilon_\perp=(\langle\varepsilon_{33}\sin^2\theta\rangle-2\langle\varepsilon_{13}\sin\theta\cos\theta\rangle+\varepsilon_{22}+\langle\varepsilon_{1_\perp}\cos^2\theta\rangle)/2 \tag{A-3}$$

The brackets $\langle\,\rangle$ denote averages over the lamellar normal directions θ and the components of ε must be included inside the brackets as they are functions of θ. Therefore, to compute the averages the distribution of θ's must be known and not just the second moment $\langle\cos^2\theta\rangle$. To accomplish this it is assumed that in:

$$\langle F(\theta)\rangle=\int_0^{\pi/2}F(\theta)\,\eta(\theta)\sin\theta\,\mathrm{d}\theta\Big/\int_0^{\pi/2}\eta(\theta)\sin\theta\,\mathrm{d}\theta$$

the distribution function $\eta(\theta)$ for lamellar surface normals is represented by the empirical function[19]:

$$\eta(\theta)=\cos^\alpha(\theta-\theta_0) \tag{A-4}$$

where θ_0 is the average tilt angle and α is a distribution parameter ($\alpha=0$ isotropic, $\to\infty$ for a narrow distribution about θ_0). It is assumed also that the crystal c-axes have the same distribution but $\theta_0=0$. Thus, α was determined from:

$$\langle\cos^2\theta_c\rangle=(\alpha+1)/(\alpha+3)$$

and the experimentally determined f_c using:

$$f_c=\tfrac{1}{2}(3\langle\cos^2\theta_c\rangle-1)$$

Lower bounds to $\varepsilon_\parallel$ and $\varepsilon_\perp$ are found by averaging the inverse of ε to find:

$$\frac{1}{\varepsilon_\parallel}=\langle\delta_{33}\cos^2\theta\rangle+2\langle\delta_{13}\sin\theta\cos\theta\rangle+\langle\delta_{11}\sin^2\theta\rangle \tag{A-5}$$

$$\frac{1}{\varepsilon_\perp}=(\langle\delta_{33}\sin^2\theta\rangle-2\langle\delta_{13}\sin\theta\cos\theta\rangle+\delta_{22}+\langle\delta_{11}\cos^2\theta\rangle)/2 \tag{A-6}$$

where δ_{11}, δ_{22}, etc. are the components of $\delta=\varepsilon^{-1}$.

To summarize, the amorphous-phase dielectric constant components ($\varepsilon_{1_\parallel}$, $\varepsilon_{1_\perp}$) were calculated as a function of θ_0, the average tilt angle, from measured values of specimen $\varepsilon_\parallel$ and $\varepsilon_\perp$ (and the known values of ε_2) using equations (A-2) and (A-3), and the adjunct relations (A-1). The averaging integrations in equations (A-2), (A-3) were carried out numerically. The solution of equations (A-2), (A-3) in terms of $\varepsilon_{1_\parallel}$, $\varepsilon_{1_\perp}$ was carried out numerically using Newton–Raphson iteration. A good starting approximation to $\varepsilon_{1_\parallel}$, $\varepsilon_{1_\perp}$ was found by combining equations (2) and (3) as $\varepsilon_\parallel+2\varepsilon_\perp$ and imposing $\varepsilon_{1_\perp}=\varepsilon_{1_\parallel}$. In this case the equations are readily solved for ε_1 analytically. Solution of the lower bound equations (A-5), (A-6) leads for the data of the present study to values of $\varepsilon_{1_\parallel}$ and $\varepsilon_{1_\perp}$ that do not differ significaly from those from equations (A-2), (A-3).